

Fixed-time Adaptive Neural Control for Physical Human-Robot Collaboration with Time-Varying Workspace Constraints

Yuzhu Sun, Mien Van*, Stephen McIlvanna, Nguyen Minh Nhat, Seán McLoone
Dariusz Ceglarek and Shuzhi Sam Ge

Abstract—Physical human-robot collaboration (pHRC) requires both compliance and safety guarantees since robots coordinate with human actions in a shared workspace. This paper presents a novel fixed-time adaptive neural control methodology for handling time-varying workspace constraints that occur in physical human-robot collaboration while also guaranteeing compliance during intended force interactions. The proposed methodology combines the benefits of compliance control, time-varying integral barrier Lyapunov function (TVIBLF) and fixed-time techniques, which not only achieve compliance during physical contact with human operators but also guarantee time-varying workspace constraints and fast tracking error convergence without any restriction on the initial conditions. Furthermore, a neural adaptive control law is designed to compensate for the unknown dynamics and disturbances of the robot manipulator such that the proposed control framework is overall fixed-time converged and capable of online learning without any prior knowledge of robot dynamics and disturbances. The proposed approach is finally validated on a simulated two-link robot manipulator. Simulation results show that the proposed controller is superior in the sense of both tracking error and convergence time compared with the existing barrier Lyapunov functions based controllers, while simultaneously guaranteeing compliance and safety.

Index Terms—Physical human-robot collaboration, fixed-time convergence, time-varying integral barrier Lyapunov functions, compliance control, robot manipulator

I. INTRODUCTION

The past few decades have seen rapid development in robot technology and its applications, which allows humans and robots to execute a variety of complex tasks in a shared workspace [1]. To guarantee safety during tasks, robots and human operators have been organised in completely separate areas. However, physical contact between humans and robots is unavoidable in some specific scenarios, such as rehabilitation robots [2] which guide a patient’s arm while coordinating with human movements with a natural fluidity, and collaborative industrial robots performing shared tasks such as holding or co-carrying a load with human partners. Three nested levels of safe human-robot collaboration are given in [3], namely: (i) *safety*, which is realized by detecting

Yuzhu Sun, Stephen McIlvanna, Nguyen Minh Nhat, Seán McLoone and Mien Van (corresponding author) are with the Centre for Intelligent Autonomous Manufacturing Systems, School of Electronics, Electrical Engineering and Computer Science, Queen’s University Belfast, Northern Ireland, UK. (email: ysun32, smcilvanna01, nnhat01, s.mcloone, m.van@qub.ac.uk)

Dariusz Ceglarek is with the Warwick Manufacturing Group, University of Warwick, Coventry, UK (email: D.J.Ceglarek@warwick.ac.uk)

Shuzhi Sam Ge is with the Department of Electrical and Computer Engineering and Social Robotics Laboratory, National University of Singapore, Singapore (email: samge@nus.edu.sg)

and isolating any unintended collisions in the presence of human operators; (ii) *coexistence*, which allows humans and robots to work in the same workspace without the coordination of actions, and; (iii) *collaboration*, which includes physical and contactless collaboration. Among these, physical collaboration requires the robot to be capable of coordinating with human motions with intended physical contacts and exchanging forces with the human in a safe way. Physical collaborative robots make full use of the reasoning capabilities of human partners, and the high precision, repeatability and heavy-duty task execution capabilities of robots [4] [5], enabling them to perform much more complicated tasks compared to traditional automated robotic systems [6]. During tasks, *coexistence* is the primary mode of operation, and *collaboration* occurs when monitoring signals generated from sensors (e.g., force/torque sensors or camera) detect the presence of physical human contacts. This raises the question of how safe physical human-robot collaboration (pHRC) can be conducted during *coexistence* whilst ensuring *compliance* during *collaboration*.

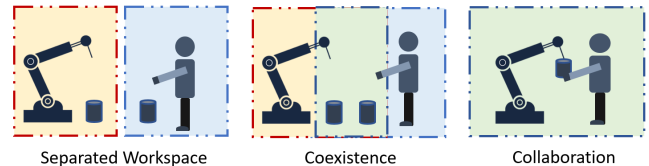


Fig. 1: Physical human-robot collaboration.

Traditional position control, whose task is to follow a specific trajectory as accurately as possible, rejects the interaction forces between the robot and human as disturbances [2]. To achieve so-called *compliance* during physical contact, there is a vast body of work on impedance/admittance based compliance control in robotics [7]–[11]. Compliance control considers both position and force in order to obtain robot movements that are smoother, softer and more human-friendly in the presence of external human forces. Therefore, in this work, we apply admittance control during *collaboration*. To be more specific, we derive the reference trajectory based on the desired task trajectory and force feedback from force/torque sensors. By following such a reference trajectory rather than the original one, robots can coordinate with human motions and comply with human forces during the intended physical contact.

Another major factor with collaborative robots that hinders their use in the real world is safety [12]. Robots are complex

and fragile. The risk of unwanted collisions between the robot and the surrounding environment (e.g., workspace boundaries, moving obstacles, etc.) exists during production, setup, and regular maintenance. Unintended physical contact can hurt humans with serious consequences. This raises the question of how safety can be strictly assured during the *coexistence* process. Barrier Lyapunov functions (BLFs) based constraint control [13]–[16], which enforces safety from the control perspective, has been one of the most effective tools for dealing with constraint problems in control systems [17]. BLFs can be generally divided into logarithmic BLFs [18] [14], tangent BLFs [19] [20], and integral BLFs [9], [21]–[24]. Compared with other types of BLFs, integral BLF (IBLF) can directly restrict system states within a certain range without transforming state constraints into error constraints [25] [26]. The design process using IBLF can therefore be greatly simplified and relaxed in terms of feasibility conditions [17]. Subsequently, time-varying IBLF (TVIBLF) [25] [26] was developed to handle time-varying constraints which are more common in many practical engineering systems since safety boundaries in the workspace are usually time-varying (e.g., when dealing with moving obstacles or a human operator) [26]. In [25], TVIBLF combined with the backstepping technique is first introduced for adaptive control of nonlinear systems. In [26], TVIBLF combined with fuzzy logic systems is introduced for a class of strict-feedback nonlinear systems.

In addition to achieving safe operation, the designer expects the control system to meet the required performance in the shortest possible time [27]. Compared with existing finite-time control results [27]–[30], the convergence time of a fixed-time controller [31] can get rid of the influence of initial conditions and be pre-designed based on parameters of the controller. Studies have shown that fixed-time convergence can produce better tracking performance and robustness to disturbances [32] [33]. Despite many advantages, only a few studies have integrated fixed-time techniques into BLFs-based constrained control [34] [35] for better tracking performance, which is essential because better tracking performance with constraints means higher working safety and efficiency of the physical human-robot collaboration. In [34], a novel fixed-time convergent time-varying BLFs-based control scheme is proposed for uncertain nonlinear systems. In [35], a nonsingular adaptive fixed-time switching control method for a class of strict-feedback nonlinear systems is proposed. So far there is little literature that integrates fixed-time techniques into TVIBLF to improve the performance and robustness of the system. Meanwhile, model-free control is a common approach within robotics control literature, since the performance of model-based controllers is dependent on the accuracy of the model. However, even for fully rigid robots, we still need to consider the uncertainties and disturbances that are not modelled such as motor/actuator errors, unintended external human forces and the influence of the noisy environment [36]. Apart from this, model-free controllers can be compatible with robotic systems which have different dynamic models, and therefore

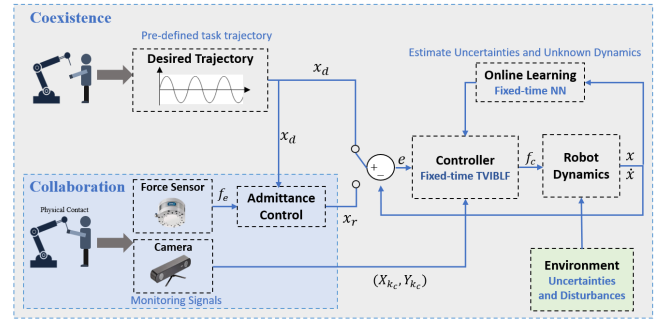


Fig. 2: The structure of proposed control framework.

be more practical in real-world scenarios. To suppress these problems, fuzzy logic systems (FLSs) [34] [37] and neural networks (NNs) [38]–[40] have long been introduced to estimate uncertainties inherent in practical systems and the influences of unknown dynamics.

Motivated by the above discussion, in this paper, a novel fixed-time control technique that integrates the fixed-time technique into the time-varying integral barrier Lyapunov function during the backstepping control design process. To eliminate the impact of unknown dynamics and model uncertainties, a novel neural network adaptive law is designed to achieve overall fixed-time convergence of the system, which further emphasises the novel contribution of this paper. The overall structure of the proposed control framework is shown in Fig. 2. The contributions and innovations of the proposed approach can be highlighted in a comparison with other approaches as follows:

- 1) Compared with existing IBLF and TVIBLF based constrained control [9] [25], the proposed controller (FxTTVIBLF) integrates the fixed-time technique into the backstepping control design process to derive a controller with fixed-time convergence. Such a controller provides better tracking performance with lower tracking error, fast convergence and higher robustness to the disturbances without any dependency on initial conditions. Meanwhile, a neural network adaptor is designed to approximate the unknown dynamics and uncertainties online such that the proposed control framework is overall fixed-time convergent and compatible with different robotic systems.
- 2) Compared with existing control methods for physical human-robot collaboration, the proposed approach guarantees the time-varying safety constraints with better tracking performance during coexistence, while simultaneously guaranteeing compliance when physical collaboration occurs. Such a controller is more practical in real-world scenarios since safety and compliance are two essential concerns that need to be addressed during physical collaboration.

The remainder of this paper is organized as follows. The general mathematical model of the robot manipulator, admittance control, neural networks and the problem formulation are presented in Section II. The design process of fixed-

time time-varying constrained control and neural network adaptor are developed in Section III. Simulation results of the proposed system are presented in Section IV. Finally, Section V discusses the conclusions and future work.

II. PROBLEM FORMULATIONS AND PRELIMINARIES

In this section, we begin by briefly introducing the dynamic model of the robot manipulator, the basics of admittance control, neural networks and overall problem formulation. In addition, some important lemmas are also given in this section, which pave the way for the control design and the proof of stability.

A. Robot Dynamic Model

The dynamic model of the robot describes the relationship between force and motion. In joint space, the dynamics of a robot manipulator can be written as:

$$M(q)\ddot{q} + C(q, \dot{q})\dot{q} + G(q) + F(q, \dot{q}) = \tau_c + \tau_e \quad (1)$$

where $q = [q_1, q_2, \dots, q_n]^T$ is the vector of joint angles, n is the number of the degree of freedom (DOF) of the robot manipulator, and \dot{q} and \ddot{q} are the joint velocities and accelerations, respectively. $M(q)$ is the mass matrix, $C(q, \dot{q})$ is the Coriolis and centrifugal forces matrix, $G(q)$ is the gravity matrix and $F(q, \dot{q})$ is the friction matrix for the manipulator. The $M(q)$, $C(q, \dot{q})$ and $G(q)$ terms contain uncertainties and $F(q, \dot{q})$ represent disturbances. τ_c is the control torque generated by the controller that we are going to design in the following sections, and τ_e is the external torque from the human operator. Employing the joint space dynamics of the robot can simplify the mathematics of the relationship between each joint of the robot. However, in real-life scenarios, the task trajectory and safety constraints for obstacles are always described in the Cartesian space. The transformation between joint angle velocities and Cartesian velocities of the robot manipulator can be written as:

$$\dot{x} = J(q)\dot{q} \quad (2)$$

where $J(q)$ is the Jacobian of the robot manipulator. To simplify the problem, we assume the Jacobian is known and non-singular in this paper. Using (2), we can transfer the joint space dynamics of the robot (1) into Cartesian space as:

$$M_x\ddot{x} + C_x\dot{x} + G_x + F_x = f_c + f_e \quad (3)$$

where $x = [x_1, x_2, \dots, x_m]^T$ is the position of the robot end-effector in Cartesian space. To simplify the problem, we assume the robot is non-redundant ($m = n$). \dot{x} and \ddot{x} are the Cartesian velocity and acceleration. $f_c = J^{-T}(q)\tau_c$, and $f_e = J^{-T}(q)\tau_e$ denote the control forces and the external human forces, respectively. The coefficient matrices transferred to Cartesian space are given as:

$$\begin{aligned} M_x &= J^{-T}(q)M(q)J^{-1}(q) \\ C_x &= J^{-T}(q)\left(C(q, \dot{q}) - M(q)J^{-1}(q)\dot{J}(q)\right)J^{-1}(q) \\ G_x &= J^{-T}(q)G(q), F_x = J^{-T}(q)F(q, \dot{q}) \end{aligned} \quad (4)$$

The following important properties pertaining to the robot dynamic equations can be exploited to good advantage for control design [41]:

Property 1: The matrix M_x is symmetric positive definite.

Property 2: The matrix $\dot{M}_x - 2C_x$ is skew symmetric.

B. Admittance Control

To provide compliance for physical human-robot force interaction, the contact point between the human and the robot is modelled as a mass-spring-damper system to imitate human muscle mechanisms. The virtual mass, spring, and damper ensure that the interaction forces are elastic and never vibrate at the contact point, as depicted in Fig. 3.

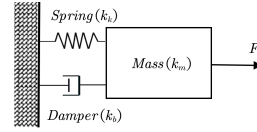


Fig. 3: Mass-spring-damper system.

Impedance and admittance are two opposite notions in compliance control. The system is regarded as admittance when the input is force and the output is position, while it is impedance when the input is position and the output is force. In this work, we are going to derive the trajectory which performs compliance behaviour based on the predefined trajectory and force feedback from force sensors. Therefore, we apply admittance control in our proposed framework. Since we need to implement Cartesian compliance, we assign the stiffness and damping at the end-effector level as follows:

$$k_{m_i}(\ddot{x}_{r_i} - \ddot{x}_{d_i}) + k_{b_i}(\dot{x}_{r_i} - \dot{x}_{d_i}) + k_{k_i}(x_{r_i} - x_{d_i}) = f_{e_i} \quad (5)$$

Here k_{m_i} , k_{b_i} and k_{k_i} are the mass, spring and damping coefficients for each dimension, $i = 1, 2, \dots, m$. x_{d_i} is the desired trajectory which is pre-defined to finish the task, and x_{r_i} is the reference trajectory which we pursue to perform compliance behaviours in response to external human forces f_{e_i} . When we define the x_{d_i} and detect the human force f_{e_i} via force sensors, x_{r_i} can be derived by integrating (5) twice.

C. Radial Basis Functions Neural Networks

Radial Basis Functions Neural Networks (RBFNNs), commonly used for function approximation problems, contain three layers: the input layer, hidden layer and output layer. The input layer consists of predictor variables $X = [x_1, x_2, \dots, x_r]^T$ which are considered to be useful or informative with respect to the output. r is the number of the input variables. The hidden layer contains a variable number of neurons $\Phi(X) = [\Phi_1(X), \Phi_2(X), \dots, \Phi_l(X)]^T$, where l is the number of hidden nodes. Each neuron comprises a Gaussian radial basis function which is defined as:

$$\Phi_i(X) = \exp\left(\frac{-(X - C_i)^T(X - C_i)}{B_i^2}\right), i = 1, 2, \dots, l \quad (6)$$

where $C_i = [c_{i1}c_{i2}, \dots, c_{ir}]^T$ is the centre and B_i is the width of i -th Gaussian radial basis functions. The output of the RBFNN is given by:

$$\hat{H}(X) = \hat{\theta}^T \Phi(X) \quad (7)$$

Here, $\hat{\theta} = [\hat{\theta}_1, \hat{\theta}_2, \dots, \hat{\theta}_l]^T$ denotes the estimation of the optimal weights θ associated with the hidden nodes. The RBFNN in (7) can approximate functions to arbitrary accuracy when the number of hidden nodes is large enough. Therefore, the optimal output $H(X)$ can be expressed as

$$H(X) = \theta^T \Phi(X) + \epsilon \quad (8)$$

where ϵ denotes the approximation error of the RBFNN. The optimal weight θ is obtained by minimizing the estimation error over the training set.

$$\theta = \underset{\theta \in \mathbb{R}^l}{\operatorname{argmin}} \left\{ \sup_{X \in \Omega_X} |H(X) - \theta^T \Phi(X)| \right\} \quad (9)$$

Assumption 1 [38]: The approximation error ϵ is bounded by $|\epsilon| \leq \bar{\epsilon}$ with the constant $\bar{\epsilon} > 0$.

D. Problem Formulation

For ease of the backstepping control design, let $\eta_1 = x, \eta_2 = \dot{x}$ and $u = f_c$. Cartesian dynamics (3) can then be written as:

$$\begin{cases} \dot{\eta}_1 = \eta_2 \\ \dot{\eta}_2 = M_x^{-1} (-C_x \eta_2 - G_x - F_x + f_e + u) \end{cases} \quad (10)$$

The control object of this paper is to make task space variable x track a desired trajectory x_d whilst complying with human force f_e . In addition, x is constrained by the time-varying workspace safety constraints $k_c(t) = [k_{c1}(t), k_{c2}(t), \dots, k_{cn}(t)]^T$ to satisfy $|x_i| \leq k_{c_i}(t)$, where $i = 1, 2, \dots, n$. The following lemmas will be useful in the control design in the next section.

Lemma 1 [42]: Consider a nonlinear system:

$$\dot{x} = f(x, t), x(0) = x_0 \quad (11)$$

where $x \in R^n$, and $f: R^n \rightarrow R^n$ is a nonlinear function. If there exists a Lyapunov function $V(x)$ such that:

$$\dot{V}(x) \leq -\alpha V^{p_c}(x) - \beta V^{q_c}(x) + \sigma \quad (12)$$

where $\alpha, \beta > 0, p_c > 1, 0 < q_c < 1$ and σ is a small positive constant, then the system (11) is practical fixed-time stable and the residual set of the system solution is given by:

$$\Omega_x = \left\{ x | V(x) \leq \min \left\{ \left[\frac{\sigma}{\alpha(1-v)} \right]^{\frac{1}{p_c}}, \left[\frac{\sigma}{\beta(1-v)} \right]^{\frac{1}{q_c}} \right\} \right\} \quad (13)$$

where v is a scalar and satisfies $0 < v \leq 1$. Then, the time T which is needed to reach the residual set is bounded by:

$$T \leq T_{\max} := \frac{1}{\alpha v(p_c - 1)} + \frac{1}{\beta v(1 - q_c)} \quad (14)$$

Lemma 2 [22]: Consider an Integral Barrier Lyapunov Functions (IBLFs) candidate:

$$V_i = \int_0^{z_{1_i}} \frac{\delta k_{c_i}^2}{k_{c_i}^2 - (\delta + x_{d_i})^2} d\delta \quad (15)$$

The function described in (15) satisfies the following property for any $|\eta_{1_i}| < k_{c_i}$:

$$V_i \leq \frac{k_{c_i}^2 z_{1_i}^2}{k_{c_i}^2 - \eta_{1_i}^2} \quad (16)$$

Lemma 3 [43]: Let $\tilde{W} = W - \hat{W}$, for any $0 < q_c < 1$, where $q_c = \frac{q_{c1}}{q_{c2}}$ and q_{c1}, q_{c2} are odd integers, the following inequality holds:

$$\tilde{W} \hat{W}^{q_c} \leq n_1 W^{q_c+1} - n_2 \tilde{W}^{q_c+1} \quad (17)$$

where $n_1 = \left(\frac{1}{1+q_c} \right) \left(1 - 2^{q_c-1} + \frac{q_c}{1+q_c} + \frac{2^{q_c}(1-q_c^2)}{1+q_c} \right)$ and $n_2 = \frac{2^{q_c-1}}{1+q_c} (1 - 2^{q_c(q_c-1)})$.

Lemma 4 [44]: For $x_i \geq 0, p_c > 1$ and $0 < q_c < 1$, the following inequalities hold:

$$\begin{aligned} n^{1-p_c} \left(\sum_{i=1}^n x_i \right)^{p_c} &\leq \sum_{i=1}^n x_i^{p_c} \\ \left(\sum_{i=1}^n x_i \right)^{q_c} &\leq \sum_{i=1}^n x_i^{q_c} \end{aligned} \quad (18)$$

Lemma 5 [45]: Let $a > 0$ be a constant and $b < a, p_c$ is an odd integer and $p_c > 1$, the following inequality holds:

$$b(a-b)^{p_c} \leq a^{p_c+1} - b^{p_c+1} \quad (19)$$

Lemma 6 [45]: Consider a differential equation of the form:

$$\dot{x}(t) = -c_1 x^{2\mu-1}(t) - c_2 x^{2\nu-1}(t) + \sigma(t) \quad (20)$$

where $x(t) \in R, c_1$ and c_2 are positive constants. $\mu = \frac{p_1}{q_1} > 1, 1 > \nu = \frac{p_2}{q_2} > \frac{1}{2}$, where p_1, p_2, q_1, q_2 are positive odd numbers and $\sigma(t)$ is a positive function. If $x(t_0) \geq 0, x(t) \geq 0$ holds for $\forall t \geq t_0$.

Lemma 7 (Young's inequality) [46]: For $\forall (x, y) \in R^2$, the following inequality holds:

$$xy \leq \frac{\varepsilon^a}{a} |x|^a + \frac{1}{b\varepsilon^b} |y|^b \quad (21)$$

where $\varepsilon > 0, a, b > 1$ and $(a-1)(b-1) = 1$.

Lemma 8 [38]: For $\forall x \in R$, the following inequality holds:

$$\lambda_{\min}(M) \|x\|^2 \leq x^T M x \leq \lambda_{\max}(M) \|x\|^2 \quad (22)$$

where $\lambda_{\min}(M)$ and $\lambda_{\max}(M)$ represents the minimum and maximum eigenvalues of M , respectively. $\|\cdot\|$ represents the Euclidean norm.

III. CONTROL DESIGN AND STABILITY ANALYSIS

In this section, we first give details of the model-based fixed-time time-varying IBLF controller design and how the backstepping method is incorporated within the design process. Then, for compatibility with different robotic systems and complex environments, we introduce NN models to approximate the uncertainties and unknown dynamics. The proposed control framework is overall fixed-time convergent. The proof of the stability and the analysis of the fixed convergence time are given subsequently. Firstly, according to (10), we define the error variables as follows:

$$\begin{aligned} z_1 &= \eta_1 - x_r \\ z_2 &= \eta_2 - \alpha \end{aligned} \quad (23)$$

where $\eta_1 = [\eta_{11}, \eta_{12}, \dots, \eta_{1n}]^T$ and $\eta_2 = [\eta_{21}, \eta_{22}, \dots, \eta_{2n}]^T$ are states of the system. $x_r = [x_{r1}, x_{r2}, \dots, x_{rn}]^T$ is the reference trajectory generated from admittance control (5). $\alpha = [\alpha_1, \alpha_2, \dots, \alpha_n]^T$ is the stabilising function to be designed. To address the constraints on η_1 , we consider the integral barrier Lyapunov candidate as follows:

$$\begin{aligned} V_1(z_1, x_r) &= \sum_{i=1}^n V_{1_i}(z_{1_i}, x_{r_i}) \\ V_{1_i}(z_{1_i}, x_{r_i}, k_{c_i}) &= \int_0^{z_{1_i}} \frac{\delta k_{c_i}^2}{k_{c_i}^2 - (\delta + x_{r_i})^2} d\delta \end{aligned} \quad (24)$$

where the variable δ is a member within the integrating range $[0, z_{1_i}]$. k_{c_i} and x_{r_i} are the i -th element of the constraints and reference trajectory, respectively. It can be seen that V_1 is positive definite and continuously differentiable. If we design a controller u such that $\dot{V}_1 \leq 0$, V_1 satisfies the decrescent condition and is bounded. Therefore, it has to be true that $|\eta_{1_i}| \neq k_{c_i}$, which means η_{1_i} remains in the region $|\eta_{1_i}| < k_{c_i}$ and the system is safe. The time-derivative of V_1 is:

$$\dot{V}_1 = \sum_{i=1}^n \frac{z_{1_i} k_{c_i}^2}{k_{c_i}^2 - \eta_{1_i}^2} \dot{z}_{1_i} + \sum_{i=1}^n \frac{\partial V_{1_i}}{\partial x_{r_i}} \dot{x}_{r_i} + \sum_{i=1}^n \frac{\partial V_{1_i}}{\partial k_{c_i}} \dot{k}_{c_i} \quad (25)$$

According to [25]:

$$\begin{aligned} \sum_{i=1}^n \frac{\partial V_{1_i}}{\partial x_{r_i}} \dot{x}_{r_i} &= \sum_{i=1}^n \dot{x}_{r_i} \int_0^{z_{1_i}} \frac{\partial}{\partial x_{r_i}} \frac{\delta k_{c_i}^2}{k_{c_i}^2 - (\delta + x_{r_i})^2} d\delta \\ &= \sum_{i=1}^n \dot{x}_{r_i} z_{1_i} \left(\frac{k_{c_i}^2}{k_{c_i}^2 - \eta_{1_i}^2} - \rho_i \right) \end{aligned} \quad (26)$$

where

$$\rho_i = \frac{k_{c_i}}{2z_{1_i}} \ln \left(\frac{(k_{c_i} + \eta_{1_i})(k_{c_i} - x_{r_i})}{(k_{c_i} - \eta_{1_i})(k_{c_i} + x_{r_i})} \right) \quad (27)$$

Similarly to (26):

$$\begin{aligned} \sum_{i=1}^n \frac{\partial V_{1_i}}{\partial k_{c_i}} \dot{k}_{c_i} &= \sum_{i=1}^n \dot{k}_{c_i} \int_0^{z_{1_i}} \frac{\partial}{\partial k_{c_i}} \frac{\delta k_{c_i}^2}{k_{c_i}^2 - (\delta + x_{r_i})^2} d\delta \\ &= \sum_{i=1}^n \dot{k}_{c_i} z_{1_i} \left(\frac{-z_{1_i} k_{c_i}}{k_{c_i}^2 - \eta_{1_i}^2} + \omega_i \right) \end{aligned} \quad (28)$$

where

$$\begin{aligned} \omega_i &= -\frac{x_{r_i} k_{c_i}}{k_{c_i}^2 - \eta_{1_i}^2} + \frac{k_{c_i}}{z_{1_i}} \ln \left(\frac{k_{c_i}^2 - \eta_{1_i}^2}{k_{c_i}^2 - x_{r_i}^2} \right) \\ &\quad + \frac{x_{r_i}}{2z_{1_i}} \ln \left(\frac{k_{c_i}^2 - x_{r_i}^2}{k_{c_i}^2 - \eta_{1_i}^2} \right) \end{aligned} \quad (29)$$

Since $\dot{z}_{1_i} = \dot{z}_{2_i} + \alpha_i - \dot{x}_{r_i}$, substitute (26)-(29) into (25), we have:

$$\begin{aligned} \dot{V}_1 &= \sum_{i=1}^n \frac{z_{1_i} z_{2_i} k_{c_i}^2}{k_{c_i}^2 - \eta_{1_i}^2} + \sum_{i=1}^n \frac{\alpha_i z_{1_i} k_{c_i}^2}{k_{c_i}^2 - \eta_{1_i}^2} + \sum_{i=1}^n \frac{-z_{1_i} k_{c_i} \dot{k}_{c_i}}{k_{c_i}^2 - \eta_{1_i}^2} \\ &\quad - \sum_{i=1}^n \frac{z_{1_i} \rho_i \dot{x}_{r_i} (k_{c_i}^2 - \eta_{1_i}^2)}{k_{c_i}^2 - \eta_{1_i}^2} + \sum_{i=1}^n \frac{z_{1_i} \omega_i \dot{k}_{c_i} (k_{c_i}^2 - \eta_{1_i}^2)}{k_{c_i}^2 - \eta_{1_i}^2} \end{aligned} \quad (30)$$

Design the stabilizing function α_i as:

$$\begin{aligned} \alpha_i &= \frac{(k_{c_i}^2 - \eta_{1_i}^2) \dot{x}_{r_i} \rho_i}{k_{c_i}^2} - \frac{(k_{c_i}^2 - \eta_{1_i}^2) \dot{k}_{c_i} \omega_i}{k_{c_i}^2} + \frac{z_{1_i} \dot{k}_{c_i}}{k_{c_i}} \\ &\quad - \theta_1 \frac{z_{1_i}^{2p_c-1} k_{c_i}^{2p_c-2}}{(k_{c_i}^2 - \eta_{1_i}^2)^{p_c+1}} - \theta_2 \frac{z_{1_i}^{2q_c-1} k_{c_i}^{2q_c-2}}{(k_{c_i}^2 - \eta_{1_i}^2)^{q_c+1}} - \kappa_{1_i} z_{1_i} \end{aligned} \quad (31)$$

where κ_1 is a positive control gain and $\theta_1, \theta_2 > 0$, $p_c > 1$, $0 < q_c < 1$. Substitute (31) into (30), we have:

$$\begin{aligned} \dot{V}_1 &= \sum_{i=1}^n \frac{z_{1_i} z_{2_i} k_{c_i}^2}{k_{c_i}^2 - \eta_{1_i}^2} - \sum_{i=1}^n \frac{\kappa_{1_i} z_{1_i}^2 k_{c_i}^2}{k_{c_i}^2 - \eta_{1_i}^2} \\ &\quad - \theta_1 \sum_{i=1}^n \left(\frac{z_{1_i}^2 k_{c_i}^2}{k_{c_i}^2 - \eta_{1_i}^2} \right)^{p_c} - \theta_2 \sum_{i=1}^n \left(\frac{z_{1_i}^2 k_{c_i}^2}{k_{c_i}^2 - \eta_{1_i}^2} \right)^{q_c} \end{aligned} \quad (32)$$

For any $|\eta_{1_i}| < k_{c_i}$, it is clear that $\sum_{i=1}^n \frac{\kappa_{1_i} z_{1_i}^2 k_{c_i}^2}{k_{c_i}^2 - \eta_{1_i}^2} > 0$. Therefore, according to Lemma 2, we have:

$$\dot{V}_1 \leq \sum_{i=1}^n \frac{z_{1_i} z_{2_i} k_{c_i}^2}{k_{c_i}^2 - \eta_{1_i}^2} - \theta_1 \sum_{i=1}^n (V_{1_i})^{p_c} - \theta_2 \sum_{i=1}^n (V_{1_i})^{q_c} \quad (33)$$

According to Lemma 4, we have:

$$\dot{V}_1 \leq \sum_{i=1}^n \frac{z_{1_i} z_{2_i} k_{c_i}^2}{k_{c_i}^2 - \eta_{1_i}^2} - \lambda_1 V_1^{p_c} - \lambda_2 V_1^{q_c} \quad (34)$$

where

$$\begin{aligned} \lambda_1 &= \theta_1 n^{1-p_c} \\ \lambda_2 &= \theta_2 \end{aligned} \quad (35)$$

Remark 1: When implementing the stabilizing function α , there will be a singularity problem when $z_1 = 0$. By using L'Hôpital's rule, we have:

$$\begin{aligned} \lim_{z_{1_i} \rightarrow 0} \rho_i &= \frac{k_{c_i}^2}{k_{c_i}^2 - x_{r_i}^2} \\ \lim_{z_{1_i} \rightarrow 0} \omega_i &= \frac{x_{r_i}^2 - 3x_{r_i} k_{c_i}}{k_{c_i}^2 - x_{r_i}^2} \end{aligned} \quad (36)$$

Then, we design the controller u to provide stability and fixed-time convergence properties to the system:

$$\begin{aligned} u &= G_x + F_x + M_x \dot{\alpha} + C_x \alpha - f_e - \frac{k_c^2 z_1}{k_c^2 - \eta_1^2} \\ &\quad - k_1 z_2 - \frac{1}{2^{p_c}} k_2 z_2^{2p_c-1} - \frac{1}{2^{q_c}} k_3 z_2^{2q_c-1} \end{aligned} \quad (37)$$

where k_1 is a positive control gain, k_2, k_3, p_c and q_c are fixed-time constants which satisfy $k_2, k_3 > 0, p_c > 1$ and $0 < q_c < 1$.

Theorem 1: Consider the system (1) subject to the constraints $k_c(t)$ and external disturbances $F(q, \dot{q})$. The system is fixed-time stable and the convergence time of the tracking errors is bounded by applying the stabilizing function (31) and the controller (37).

Proof: Select a Lyapunov function candidate as:

$$V_2 = \frac{1}{2} z_2^T M_x z_2 \quad (38)$$

According to Property 1, Property 2, (10) and (23), the time derivative of V_2 is:

$$\begin{aligned} \dot{V}_2 &= z_2^T M_x \dot{z}_2 + \frac{1}{2} z_2^T \dot{M}_x z_2 = z_2^T (M_x \dot{z}_2 + C_x z_2) \\ &= z_2^T (u + f_e - G_x - F_x - M_x \dot{\alpha} - C_x \alpha) \end{aligned} \quad (39)$$

Inserting the controller (37) into (39), according to Lemma 4 and Lemma 8, we have:

$$\begin{aligned} \dot{V}_2 &= z_2^T \left(-\frac{k_c^2 z_1}{k_c^2 - \eta_1^2} - k_1 z_2 - \frac{1}{2^{p_c}} k_2 z_2^{2p_c-1} - \frac{1}{2^{q_c}} k_3 z_2^{2q_c-1} \right) \\ &\leq -\sum_{i=1}^n \frac{z_{1_i} z_{2_i} k_{c_i}^2}{k_{c_i}^2 - \eta_{1_i}^2} - \lambda_{\min}(k_2) n^{1-p_c} \left(\frac{1}{2} \|z_2\|^2 \right)^{p_c} \\ &\quad - \lambda_{\min}(k_3) \left(\frac{1}{2} \|z_2\|^2 \right)^{q_c} \end{aligned} \quad (40)$$

Therefore, we have:

$$\begin{aligned} \dot{V}_2 &\leq -\sum_{i=1}^n \frac{z_{1_i} z_{2_i} k_{c_i}^2}{k_{c_i}^2 - \eta_{1_i}^2} - \frac{\lambda_{\min}(k_2)}{\lambda_{\max}(M)^{p_c}} n^{1-p_c} \left(\frac{1}{2} z_2^T M z_2 \right)^{p_c} \\ &\quad - \frac{\lambda_{\min}(k_3)}{\lambda_{\max}(M)^{q_c}} \left(\frac{1}{2} z_2^T M z_2 \right)^{q_c} \\ &= -\sum_{i=1}^n \frac{z_{1_i} z_{2_i} k_{c_i}^2}{k_{c_i}^2 - \eta_{1_i}^2} - \lambda_3 V_2^{p_c} - \lambda_4 V_2^{q_c} \end{aligned} \quad (41)$$

where

$$\begin{aligned} \lambda_3 &= \frac{\lambda_{\min}(k_2)}{\lambda_{\max}(M)^{p_c}} n^{1-p_c} \\ \lambda_4 &= \frac{\lambda_{\min}(k_3)}{\lambda_{\max}(M)^{q_c}} \end{aligned} \quad (42)$$

Therefore, according to Lemma 4, the derivative of the Lyapunov function for the proposed controller is:

$$\begin{aligned} \dot{V} &= \dot{V}_1 + \dot{V}_2 \leq -\lambda_1 V_1^{p_c} - \lambda_2 V_1^{q_c} - \lambda_3 V_2^{p_c} - \lambda_4 V_2^{q_c} \\ &\leq -v_1 V^{p_c} - v_2 V^{q_c} \end{aligned} \quad (43)$$

where

$$\begin{aligned} v_1 &= 2^{1-p_c} \min(\lambda_1, \lambda_3) \\ v_2 &= \min(\lambda_2, \lambda_4) \end{aligned} \quad (44)$$

According to Lemma 1, the proposed controller u is fixed-time stable. Assuming the robot dynamics are unknown. In the controller u defined in (37), we collect the terms that contains dynamics and disturbances into a function $D(Z) \in R^n$, and then design NNs to approximate it, that is:

$$D(Z) = -G_x - F_x - M_x \dot{\alpha} - C_x \alpha = W^T S(Z) + \epsilon \quad (45)$$

Each joint of the robot manipulator is assigned it own NN for approximation, hence, $D(Z) = [D_1(Z_1), D_2(Z_2), \dots, D_n(Z_n)]^T$. The i -th element of $D(Z)$ is given by:

$$D_i(Z_i) = W_i^T S_i(Z_i) + \epsilon_i \quad (46)$$

where $Z_i = [z_{i1}, z_{i2}, \dots, z_{ir}]^T$, $W_i = [w_{i1}, w_{i2}, \dots, w_{il}]^T$, and $S_i(Z_i) = [s_{i1}(Z_i), s_{i2}(Z_i), \dots, s_{il}(Z_i)]^T$ are the input vector, weight vector and hidden layer output of the i -th NN, respectively. Each hidden node comprises a Gaussian radial basis function s_{ii} as defined in (6), and $Z_i = [q_1, \dots, q_n, \dot{q}_1, \dots, \dot{q}_n, \alpha_1, \dots, \alpha_n, \dot{\alpha}_1, \dots, \dot{\alpha}_n]^T$ is the vector of input variables. To enable a compact matrix representation, in (45), $W \in R^{n \times nl}$ is defined as $W = \text{diag}[W_1^T, W_2^T, \dots, W_n^T]$ and $S(Z) \in R^{nl \times 1}$ is defined as $S = [S_1, S_2, \dots, S_n]^T$. $\epsilon = [\epsilon_1, \epsilon_2, \dots, \epsilon_n]^T$ is the vector of the estimation errors of each joint.

Denoting \hat{W}_i as the estimate of W_i , and the estimation error as $\tilde{W}_i = W_i - \hat{W}_i$, we design the adaptive NN update law as:

$$\dot{\hat{W}}_i = S_i(Z_i) z_{2_i} - k_4 \hat{W}_i^{2p_c-1} - k_5 \hat{W}_i^{2q_c-1} \quad (47)$$

By using NNs, the formulation of controller u becomes:

$$\begin{aligned} u &= -\hat{W}^T S(Z) - f_e - \frac{k_c^2 z_1}{k_c^2 - \eta_1^2} - k_1 z_2 \\ &\quad - \frac{1}{2^{p_c}} k_2 z^{2p_c-1} - \frac{1}{2^{q_c}} k_3 z^{2q_c-1} \end{aligned} \quad (48)$$

Remark 2: The differences between the proposed NN adaptive law and the traditional adaptive laws [9] [38] are that the extra terms added at the end of the formula can ensure the overall fixed-time stability of the control system.

Remark 3: When implementing the proposed adaptive law (47), to avoid the singularity problem when $\hat{W}_i < 0$, we can replace the $-k_4 \hat{W}_i^{2p_c-1}$ term with $-k_4 \text{sign}(\hat{W}_i) |\hat{W}_i|^{2p_c-1}$ (similar to the controller u).

Theorem 2: Consider the system (1) subject to the constraints $k_c(t)$, external disturbances $F(q, \dot{q})$ and unknown dynamics $M(q)$, $C(q, \dot{q})$ and $G(q)$, the system is overall fixed-time stable and the convergence time of the tracking errors are bounded by applying the stabilizing function (31), controller (48) and the NNs adaptive law (47).

Proof: Select a Lyapunov function candidate V_3 as:

$$V_3 = \frac{1}{2} \sum_{i=1}^n \tilde{W}_i^T \tilde{W}_i \quad (49)$$

The derivative of V_3 is:

$$\begin{aligned} \dot{V}_3 &= -\sum_{i=1}^n \tilde{W}_i^T \dot{\tilde{W}}_i \\ &= \sum_{i=1}^n \tilde{W}_i^T \left(-S_i(Z) z_{2_i} + k_4 \hat{W}_i^{2p_c-1} + k_5 \hat{W}_i^{2q_c-1} \right) \\ &= \sum_{i=1}^n -\tilde{W}_i^T S_i(Z) z_{2_i} + k_4 \sum_{i=1}^n \tilde{W}_i^T \hat{W}_i^{2p_c-1} + k_5 \sum_{i=1}^n \tilde{W}_i^T \hat{W}_i^{2q_c-1} \end{aligned} \quad (50)$$

According to Lemma 3, we have:

$$\tilde{W}_i \hat{W}_i^{2q_c-1} \leq n_1 W_i^{2q_c} - n_2 \tilde{W}_i^{2q_c} \quad (51)$$

Furthermore, according to Lemma 6, $\hat{W}(t) \geq 0$ is true if $\hat{W}(t_0) \geq 0$. Since $\tilde{W} = W - \hat{W}$, it is clear that $\tilde{W} \leq W$. Therefore, according to Lemma 5, we have:

$$\begin{aligned} \tilde{W}_i \hat{W}_i^{2p_c-1} &= \tilde{W}_i \left(W_i - \tilde{W}_i \right)^{2p_c-1} \\ &\leq W_i^{2p_c} - \tilde{W}_i^{2p_c} \end{aligned} \quad (52)$$

Applying Lemma 4, we obtain:

$$\begin{aligned} \dot{V}_3 &\leq - \sum_{i=1}^n \tilde{W}_i^T S_i(Z_i) z_{2i} + k_4 \sum_{i=1}^n \sum_{j=1}^l (w_{ij}^{2p_c} - \tilde{w}_{ij}^{2p_c}) \\ &\quad + k_5 \sum_{i=1}^n \sum_{j=1}^l (n_1 w_{ij}^{2q_c} - n_2 \tilde{w}_{ij}^{2q_c}) \\ &= - \sum_{i=1}^n \tilde{W}_i^T S_i(Z_i) z_{2i} - k_4 \sum_{i=1}^n \sum_{j=1}^l \tilde{w}_{ij}^{2p_c} \\ &\quad - k_5 n_2 \sum_{i=1}^n \sum_{j=1}^l \tilde{w}_{ij}^{2q_c} + \sigma \end{aligned} \quad (53)$$

where

$$\sigma = k_4 \sum_{i=1}^n \sum_{j=1}^l w_{ij}^{2p_c} + k_5 n_1 \sum_{i=1}^n \sum_{j=1}^l w_{ij}^{2q_c} \quad (54)$$

Again, using Lemma 4, we have:

$$\begin{aligned} \dot{V}_3 &\leq - \sum_{i=1}^n \tilde{W}_i^T S_i(Z_i) z_{2i} - k_4 l^{1-p_c} \sum_{i=1}^n \left(\sum_{j=1}^l \tilde{w}_{ij}^2 \right)^{p_c} \\ &\quad - k_5 n_2 \sum_{i=1}^n \left(\sum_{j=1}^l \tilde{w}_{ij}^2 \right)^{q_c} + \sigma \\ &= - \sum_{i=1}^n \tilde{W}_i^T S_i(Z_i) z_{2i} - 2_c^p k_4 l^{1-p_c} \frac{1}{2^{p_c}} \sum_{i=1}^n \left(\tilde{W}_i^T \tilde{W}_i \right)^{p_c} \\ &\quad - 2_c^q k_5 n_2 \frac{1}{2^{q_c}} \sum_{i=1}^n \left(\tilde{W}_i^T \tilde{W}_i \right)^{q_c} + \sigma \\ &\leq - \sum_{i=1}^n \tilde{W}_i^T S_i(Z_i) z_{2i} - \lambda_5 \left(\frac{1}{2} \sum_{i=1}^n \tilde{W}_i^T \tilde{W}_i \right)^{p_c} \\ &\quad - \lambda_6 \left(\frac{1}{2} \sum_{i=1}^n \tilde{W}_i^T \tilde{W}_i \right)^{q_c} + \sigma \end{aligned} \quad (55)$$

Therefore, it follows that:

$$\dot{V}_3 \leq - \sum_{i=1}^n \tilde{W}_i^T S_i(Z_i) z_{2i} - \lambda_5 V_3^{p_c} - \lambda_6 V_3^{q_c} + \sigma \quad (56)$$

where

$$\begin{aligned} \lambda_5 &= 2^{p_c} k_4 l^{1-p_c} n^{1-p_c} \\ \lambda_6 &= 2^{q_c} k_5 n_2 \end{aligned} \quad (57)$$

Inserting the controller (48) into \dot{V}_2 gives:

$$\dot{V}_2 \leq z_2^T \tilde{W}^T S(Z) - \sum_{i=1}^n \frac{z_{1i} z_{2i} k_{c_i}^2}{k_{c_i}^2 - \eta_{1i}^2} - \lambda_3 V_2^{p_c} - \lambda_4 V_2^{q_c} - z_2^T \epsilon \quad (58)$$

According to Lemma 7 and Assumption 1:

$$-z_2^T \epsilon \leq \frac{1}{2} z_2^T z_2 + \frac{1}{2} \|\bar{\epsilon}\|^2 \quad (59)$$

Therefore:

$$\begin{aligned} \dot{V}_2 &\leq z_2^T \tilde{W}^T S(Z) - \sum_{i=1}^n \frac{z_{1i} z_{2i} k_{c_i}^2}{k_{c_i}^2 - \eta_{1i}^2} - z_2^T \left(k_1 - \frac{1}{2} I \right) z_2 \\ &\quad - \lambda_3 V_2^{p_c} - \lambda_4 V_2^{q_c} + \frac{1}{2} \|\bar{\epsilon}\|^2 \end{aligned} \quad (60)$$

where k_1 is a parameter matrix to be designed such that $k_1 - \frac{1}{2} I$ is positive. Letting $V = V_1 + V_2 + V_3$, according to (34), (60) and (56), we can write:

$$\begin{aligned} \dot{V} &\leq -\lambda_1 V_1^{p_c} - \lambda_2 V_1^{q_c} - \lambda_3 V_2^{p_c} - \lambda_4 V_2^{q_c} - \lambda_5 V_3^{p_c} - \lambda_6 V_3^{q_c} \\ &\leq -\alpha V^{p_c} - \beta V^{q_c} + \sigma \end{aligned} \quad (61)$$

where

$$\begin{aligned} \alpha &= 3^{1-p_c} \min(\lambda_1, \lambda_3, \lambda_5) \\ \beta &= \min(\lambda_2, \lambda_4, \lambda_6) \end{aligned} \quad (62)$$

and therefore by employing Lemma 1, the proposed controller combined with NNs is fixed-time stable, and that the convergence time of its tracking error is bounded by:

$$T \leq T_{\max} := \frac{1}{\alpha v (p_c - 1)} + \frac{1}{\beta v (1 - q_c)} \quad (63)$$

IV. SIMULATION EXAMPLE

In this section, a comparative simulation based on a two-link planar robot manipulator is employed to show the performance of the proposed method, as depicted in Fig. 4. The proposed method can in principle be extended to robots with arbitrary degrees of freedom.

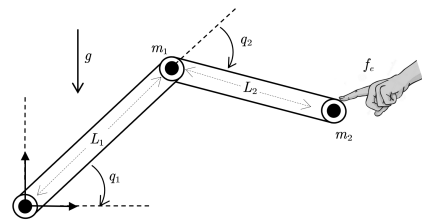


Fig. 4: A two-link planar robot manipulator.

The dynamics of the robot are given by [47]:

$$\begin{aligned} \tau_1 &= m_2 l_2^2 (\ddot{q}_1 + \ddot{q}_2) + m_2 l_1 l_2 c_2 (2\dot{q}_1 + \dot{q}_2) + (m_1 + m_2) l_1^2 \ddot{q}_1 - \\ &\quad m_2 l_1 l_2 s_2 \dot{q}_2^2 - 2m_2 l_1 l_2 s_2 \dot{q}_1 \dot{q}_2 + m_2 l_2 g c_{12} + (m_1 + m_2) l_1 g c_1 \\ \tau_2 &= m_2 l_1 l_2 c_2 \ddot{q}_1 + m_2 l_1 l_2 s_2 \dot{q}_1^2 + m_2 l_2 g c_{12} + m_2 l_2^2 (\ddot{q}_1 + \ddot{q}_2) \end{aligned}$$

where $c_i = \cos(q_i)$, $c_{ij} = \cos(q_i + q_j)$, $s_i = \sin(q_i)$, and $s_{ij} = \sin(q_i + q_j)$, $i, j = 1, 2$. The coefficient matrices $M(q)$, $C(q, \dot{q})$, and $G(q)$ are given as:

$$M(q) = \begin{bmatrix} m_2 l_2^2 + 2m_2 l_1 l_2 c_2 + (m_1 + m_2) l_1^2 & m_2 l_2^2 + m_2 l_1 l_2 c_2 \\ m_2 l_2^2 + m_2 l_1 l_2 c_2 & m_2 l_2^2 \end{bmatrix}$$

$$C(q, \dot{q}) = \begin{bmatrix} -2m_2 l_1 l_2 s_2 \dot{q}_2 & -m_2 l_1 l_2 s_2 \\ m_2 l_1 l_2 s_2 \dot{q}_1 & 0 \end{bmatrix}$$

$$G(q) = \begin{bmatrix} m_2 l_2 g c_{12} + (m_1 + m_2) l_1 g c_1 \\ m_2 l_2 g c_{12} \end{bmatrix}$$

and the uncertainties and disturbances term is defined as:

$$F(q, \dot{q}) = \begin{bmatrix} 4c_1 s_2 + 6c_1^2 - 2 \\ -4c_1 s_2 - 6c_1^2 + 2 \end{bmatrix}$$

The Jacobian of the robot is given by:

$$J(q) = \begin{bmatrix} -l_1 s_1 - l_2 s_{12} & -l_2 s_{12} \\ l_1 c_1 + l_2 c_{12} & l_2 c_{12} \end{bmatrix}$$

External human forces f_{e_i} are applied to each link of the robot at 20s and removed at 31s with profiles as specified in (64). Here, $a = [a_1, a_2]$ are link specific force scaling parameters. Fig. 5 shows the evolution of the applied forces over time.

$$f_{e_i}(t) = \begin{cases} 0 & t < 20 \text{ or } t \geq 31 \\ a_i (1 - \cos \pi t) & 20 \leq t < 21 \\ 2a_i & 21 \leq t < 30 \\ a_i (1 + \cos \pi t) & 30 \leq t < 31 \end{cases} \quad (64)$$

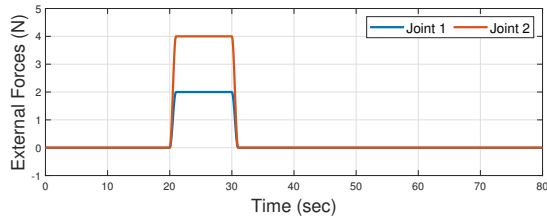


Fig. 5: External human forces.

The designed trajectory is given as:

$$\begin{aligned} x_{d_1}(t) &= 0.18 \cos(0.5t) \\ x_{d_2}(t) &= 0.18 \sin(0.5t) \end{aligned} \quad (65)$$

When we have x_{d_i} and f_{e_i} , the reference trajectory which can comply with human forces is derived by integrating (5) twice, as depicted in Fig. 6. The x_d and x_r coincide when $f_e = 0$. When $20 < t < 31$, the desired trajectory is modified by the external forces to comply with human forces.

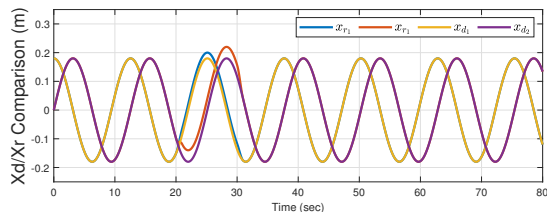


Fig. 6: Comparison of desired and reference trajectory.

TABLE I: Simulation parameters

Modules	Parameters
Initial values	$q(0) = [0.5236, 2.0944]^T$ $x(0) = [0, 0]^T$
Robot dynamics	$m_1 = 1.5kg, m_2 = 1.0kg$ $l_1 = l_2 = 0.3m$
Admittance control	$k_{m_i} = 20, k_{b_i} = 20, k_{k_i} = 100$ $a_1 = 1, a_2 = 2$ $p_c = 3, q_c = \frac{99}{101}$
Controller	$\theta_1 = [10, 0.01], \theta_2 = [20, 0.01], \kappa_1 = [5, 22]$ $k_1 = \text{diag}[5, 22], k_2 = \text{diag}[100, 2000]$ $k_3 = \text{diag}[200, 3000], k_4 = k_5 = 0.001$
NNs	$l = 8, Z = [q_1, q_2, \dot{q}_1, \dot{q}_2, \alpha_1, \alpha_2, \dot{\alpha}_1, \dot{\alpha}_2]^T$ $C = [-25, -15, -5, -1, 1, 5, 15, 25], B = 40$

The time-varying workspace safety constraints are given as:

$$\begin{aligned} k_{c_1} &= 0.48 + 0.1 \cos\left(0.2t - \frac{\pi}{3}\right) \\ k_{c_2} &= -0.48 + 0.1 \sin(0.2t) \end{aligned} \quad (66)$$

To verify the performance of the proposed controller FxTTVIBLF, we compare it with IBLF [9] and traditional TVIBLF based controllers without fixed-time terms [25]. To further illustrate the effectiveness of the proposed NNs, we divide the simulation into two cases: model-based and model-free.

Remark 4: Since there is no existing literature on TVIBLF published in the area of robot manipulators, to illustrate the improvement of the proposed fixed-time controller, the TVIBLF we applied in the comparative simulation is a simplified version of the controller proposed in this paper. That is, we delete the fixed-time terms in the proposed controller. For details of TVIBLF controller design see [25].

A. Model-based control

First, we assume all of the robot dynamics are known except for disturbances term $F(q, \dot{q})$. The parameters of the robot dynamics and proposed controller are given in Table I. Fig. 7 shows the task space trajectories of the compared controllers. We can see that the proposed FxTTVIBLF can follow the reference x_r within the time-varying constraint bounds. Moreover, the tracking accuracy of the proposed controller is better than achieved with IBLF and TVIBLF based controllers, which means the proposed controller has the best immunity to uncertainties and tracking performance is improved by integrating fixed-time terms. The RMSE tracking performance of each controller is shown in Table II.

B. Model-free control

Here we assume that all the parameters of the robot dynamics are unknown. We employ an NN (with traditional adaptive law [9]) with IBLF and TVIBLF for the contrast simulation, and employ an NN (with our proposed adaptive

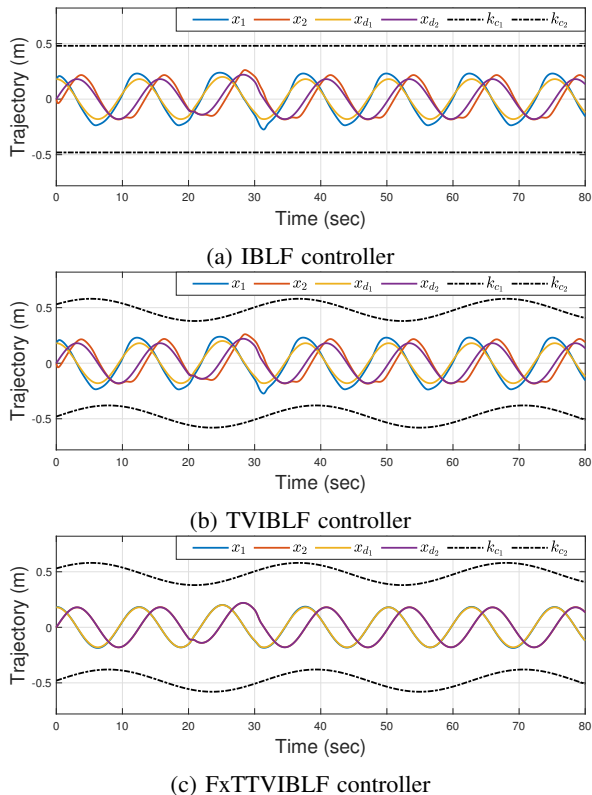


Fig. 7: Trajectories of compared controllers without NNs

law (47)) with FxTTVIBLF (48) to achieve overall fixed-time stability. By doing so, the three controllers are capable of estimating the uncertainties along with the dynamics. Fig. 8 shows the tracking trajectories of the controllers. We can see the performance of all these controllers is improved to some extent. Notably, the trajectory of the proposed FxTTVIBLF controller coincides with x_r much more quickly than observed with the other controllers, which is a consequence of the overall faster converge properties of the fixed-time control law combining with the proposed NNs adaptive law.

Fig. 9 shows the tracking errors of the various model-based and model-free controllers considered. The errors of the IBLF and TVIBLF based controllers combined with traditional NNs show chattering at the beginning and gradually converge after 40s. It is evident that the proposed controller achieves a smoother trajectory, smaller tracking error and overall faster convergence time than the other controllers. Fig. 10 shows the evolution of the NN weights vectors of the proposed FxTTVIBLF. All weights of the hidden nodes are initialized as zero at 0s and updated in real time. Table II compares the tracking RMSE performance of each controller. It is clear that the tracking performance of IBLF and TVIBLF is similar. The tracking error is smaller when we apply NNs and integrate fixed-time techniques into the control design. Fig. 11 shows the control effort of each controller. It can be seen that the proposed controller generally requires a similar control effort despite the demonstrated performance advantages over the other controllers. However, it is noted

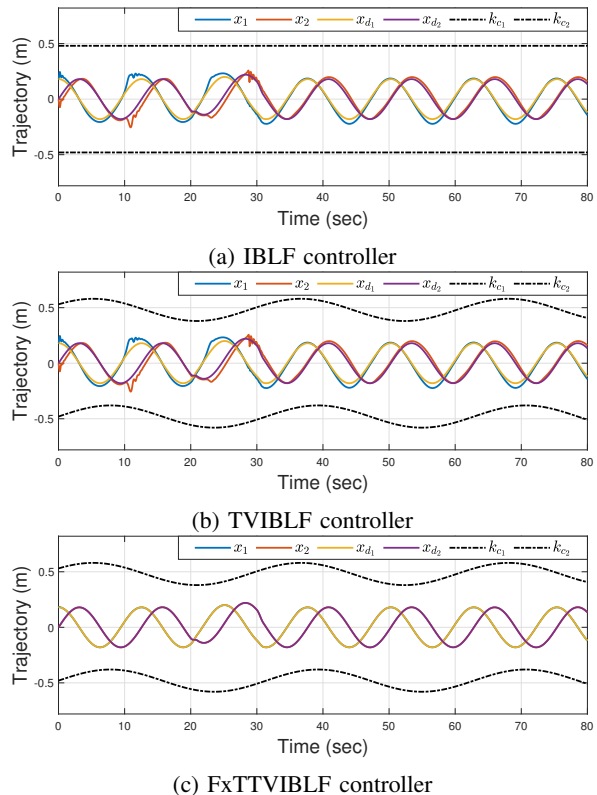


Fig. 8: Trajectories of compared controllers with NNs

TABLE II: RMSE tracking performance of each controller

Joint	IBLF	TVIBLF	FxTTVIBLF
1	3.74×10^{-2}	3.73×10^{-2}	3.2×10^{-3}
2	4.68×10^{-2}	4.69×10^{-2}	8.63×10^{-4}
Joint	IBLF+NN	TVIBLF+NN	FxTTVIBLF+NN
1	2.56×10^{-2}	2.56×10^{-2}	6.10×10^{-4}
2	2.7359×10^{-2}	2.74×10^{-2}	7.71×10^{-4}

that some chattering occurs with FxTTVIBLFs when the external forces are applied and removed (at 20s and 30s).

V. CONCLUSIONS

In this paper, a fixed-time time-varying IBLF controller based on admittance control has been proposed for physical human-robot collaboration. The proposed approach guarantees both safety and compliance during physical contact. Compared with existing methods, the proposed controller has lower tracking error, faster convergence time and more human-friendly behaviour which makes it more practical in real-life scenarios. The BLF based constraint control strictly guarantees that the resultant trajectory never violates the preset bounds. When the desired trajectory traverses beyond these bounds the robot will stop because the nature of the BLF. In the future we will build on this work and explore

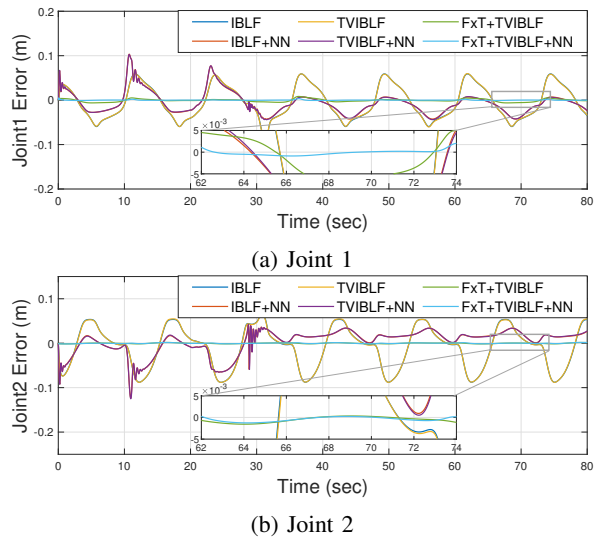


Fig. 9: Tracking errors of compared controllers

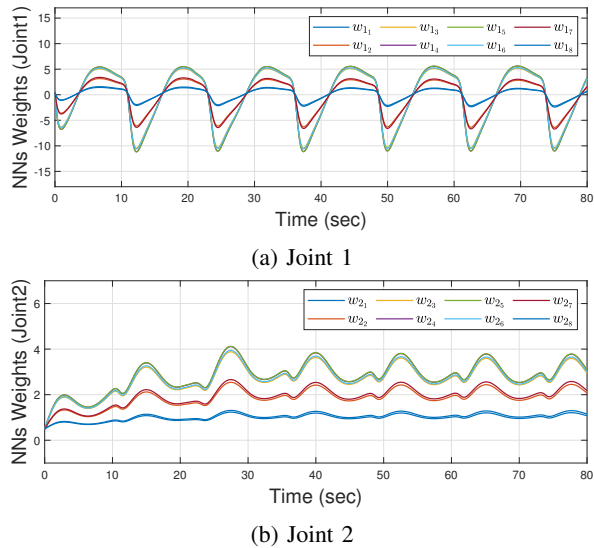


Fig. 10: NNs weights evolution of FxTTVIBLF+NN

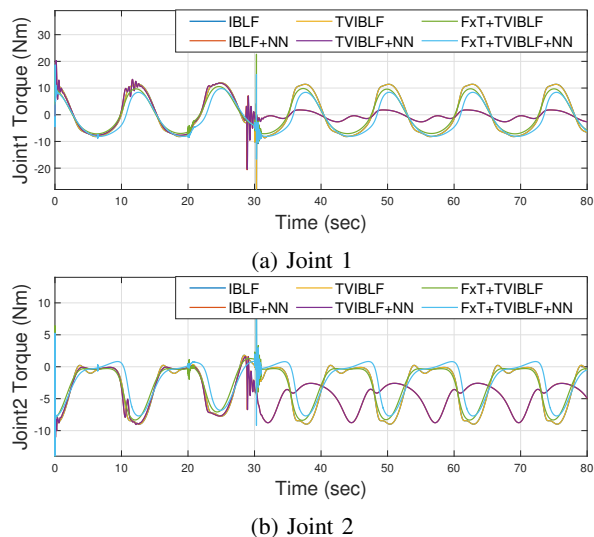


Fig. 11: Control effort of compared controllers

its use with a high-level path planning block to allow the system to achieve real time dynamic obstacle avoidance. In this context the proposed FxTTVIBLF controller will act as the low level controller to strictly guarantee safety.

REFERENCES

- [1] E. Magrini, F. Ferraguti, A. J. Ronga, F. Pini, A. De Luca, and F. Leali, "Human-robot coexistence and interaction in open industrial cells," *Robotics and Computer-Integrated Manufacturing*, vol. 61, 2020.
- [2] K. P. Tee, R. Yan, and H. Li, "Adaptive admittance control of a robot manipulator under task space constraint," in *2010 IEEE International Conference on Robotics and Automation*. IEEE, Conference Proceedings, pp. 5181–5186.
- [3] E. Magrini, F. Ferraguti, A. J. Ronga, F. Pini, A. De Luca, and F. Leali, "Human-robot coexistence and interaction in open industrial cells," *Robotics and Computer-Integrated Manufacturing*, vol. 61, 2020.
- [4] L. Wang, S. Liu, H. Liu, and X. V. Wang, *Overview of Human-Robot Collaboration in Manufacturing*, ser. Lecture Notes in Mechanical Engineering, 2020, book section Chapter 2, pp. 15–58.
- [5] V. Villani, F. Pini, F. Leali, and C. Secchi, "Survey on human-robot collaboration in industrial settings: Safety, intuitive interfaces and applications," *Mechatronics*, vol. 55, pp. 248–266, 2018.
- [6] J. Heinzmann and A. Zelinsky, "Quantitative safety guarantees for physical human-robot interaction," *The International Journal of Robotics Research*, vol. 22, no. 7-8, pp. 479–504, 2003.
- [7] E. Mariotti, E. Magrini, and A. D. Luca, "Admittance control for human-robot interaction using an industrial robot equipped with a ft sensor," in *2019 International Conference on Robotics and Automation (ICRA)*, Conference Proceedings, pp. 6130–6136.
- [8] M. Sharifi, V. Azimi, V. K. Mushahwar, and M. Tavakoli, "Impedance learning-based adaptive control for human-robot interaction," *IEEE Transactions on Control Systems Technology*, pp. 1–14, 2021.
- [9] W. He, C. Xue, X. Yu, Z. Li, and C. Yang, "Admittance-based controller design for physical human-robot interaction in the constrained task space," *IEEE Transactions on Automation Science and Engineering*, vol. 17, no. 4, pp. 1937–1949, 2020.
- [10] Z. Li, B. Huang, Z. Ye, M. Deng, and C. Yang, "Physical human-robot interaction of a robotic exoskeleton by admittance control," *IEEE Transactions on Industrial Electronics*, vol. 65, no. 12, pp. 9614–9624, 2018.
- [11] D. Engelbrecht, N. Steyn, and K. Djouani, "Adaptive virtual impedance control of a mobile multi-robot system," *Robotics*, vol. 10, p. 19, 2021.
- [12] J. Arents, V. Abolins, J. Judvaitis, O. Vismanis, A. Oraby, and K. Ozols, "Human-robot collaboration trends and safety aspects: A systematic review," *Journal of Sensor and Actuator Networks*, vol. 10, no. 3, 2021.
- [13] K. B. Ngo, R. Mahony, and Z.-P. Jiang, "Integrator backstepping using barrier functions for systems with multiple state constraints," in *Proceedings of the 44th IEEE Conference on Decision and Control*. IEEE, 2005, pp. 8306–8312.
- [14] K. P. Tee, S. S. Ge, and E. H. Tay, "Barrier lyapunov functions for the control of output-constrained nonlinear systems," *Automatica*, vol. 45, no. 4, pp. 918–927, 2009.
- [15] B. Ren, S. S. Ge, K. P. Tee, and T. H. Lee, "Adaptive neural control for output feedback nonlinear systems using a barrier lyapunov function," *IEEE Transactions on Neural Networks*, vol. 21, no. 8, pp. 1339–1345, 2010.
- [16] W. Sun, S.-F. Su, Y. Wu, J. Xia, and V.-T. Nguyen, "Adaptive fuzzy control with high-order barrier lyapunov functions for high-order uncertain nonlinear systems with full-state constraints," *IEEE Transactions on Cybernetics*, vol. 50, no. 8, pp. 3424–3432, 2020.
- [17] T. Gao, T. Li, Y. J. Liu, and S. Tong, "Iblf-based adaptive neural control of state-constrained uncertain stochastic nonlinear systems," *IEEE Transactions on Neural Networks and Learning Systems*, pp. 1–12, 2021.
- [18] D.-P. Li, Y.-J. Liu, S. Tong, C. L. P. Chen, and D.-J. Li, "Neural networks-based adaptive control for nonlinear state constrained systems with input delay," *IEEE Transactions on Cybernetics*, vol. 49, no. 4, pp. 1249–1258, 2019.
- [19] Y. Li, J. Zhang, W. Liu, and S. Tong, "Observer-based adaptive optimized control for stochastic nonlinear systems with input and state constraints," *IEEE Transactions on Neural Networks and Learning Systems*, 2021.

- [20] C. Hua, R. Meng, K. Li, and X. Guan, "Full state constraints-based adaptive tracking control for uncertain nonlinear stochastic systems with input saturation," *Journal of the Franklin Institute*, vol. 357, no. 9, pp. 5125–5142, 2020.
- [21] S. S. Ge, C. C. Hang, and T. Zhang, "Stable adaptive control for nonlinear multivariable systems with a triangular control structure," *IEEE Transactions on Automatic Control*, vol. 45, no. 6, pp. 1221–1225, 2000.
- [22] K. P. Tee and S. S. Ge, "Control of state-constrained nonlinear systems using integral barrier lyapunov functionals," in *2012 IEEE 51st IEEE Conference on Decision and Control (CDC)*, Conference Proceedings, pp. 3239–3244.
- [23] F. Yuan, Y. J. Liu, L. Liu, J. Lan, D. Li, S. Tong, and C. L. P. Chen, "Adaptive neural consensus tracking control for nonlinear multiagent systems using integral barrier lyapunov functionals," *IEEE Transactions on Neural Networks and Learning Systems*, pp. 1–11, 2021.
- [24] Z.-L. Tang, S. S. Ge, K. P. Tee, and W. He, "Adaptive neural control for an uncertain robotic manipulator with joint space constraints," *International Journal of Control*, vol. 89, no. 7, pp. 1428–1446, 2016.
- [25] L. Liu, T. Gao, Y.-J. Liu, S. Tong, C. L. P. Chen, and L. Ma, "Time-varying blfbs-based adaptive control of uncertain nonlinear systems with full state constraints," *Automatica*, vol. 129, p. 109595, 2021.
- [26] T. Yu, Y. J. Liu, L. Liu, and S. Tong, "Adaptive fuzzy control of nonlinear systems with function constraints based on time-varying blfbs," *IEEE Transactions on Fuzzy Systems*, pp. 1–1, 2022.
- [27] Y. Zhang, J. Guo, and Z. Xiang, "Finite-time adaptive neural control for a class of nonlinear systems with asymmetric time-varying full-state constraints," *IEEE Trans Neural Netw Learn Syst*, vol. PP, 2022.
- [28] L. Liu, T. Gao, Y.-J. Liu, and S. Tong, "Time-varying asymmetrical blfbs based adaptive finite-time neural control of nonlinear systems with full state constraints," *IEEE/CAA Journal of Automatica Sinica*, vol. 7, no. 5, p. 1335, 2020.
- [29] Y. Li, B. Niu, G. Zong, J. Zhao, and X. Zhao, "Command filter-based adaptive neural finite-time control for stochastic nonlinear systems with time-varying full-state constraints and asymmetric input saturation," *International Journal of Systems Science*, vol. 53, no. 1, pp. 199–221, 2021.
- [30] G. Li, X. Chen, J. Yu, and J. Liu, "Adaptive neural network-based finite-time impedance control of constrained robotic manipulators with disturbance observer," *IEEE Transactions on Circuits and Systems II: Express Briefs*, pp. 1–1, 2021.
- [31] X. Yuan, B. Chen, and C. Lin, "Neural adaptive fixed-time control for nonlinear systems with full-state constraints," *IEEE Trans Cybern*, vol. PP, 2021.
- [32] Z. Zuo, B. Tian, M. Defoort, and Z. Ding, "Fixed-time consensus tracking for multiagent systems with high-order integrator dynamics," *IEEE Transactions on Automatic Control*, vol. 63, no. 2, pp. 563–570, 2018.
- [33] M. Van and D. Ceglarek, "Robust fault tolerant control of robot manipulators with global fixed-time convergence," *Journal of the Franklin Institute*, vol. 358, no. 1, pp. 699–722, 2021.
- [34] J. Sun, J. Yi, and Z. Pu, "Fixed-time adaptive fuzzy control for uncertain nonstrict-feedback systems with time-varying constraints and input saturations," *IEEE Transactions on Fuzzy Systems*, vol. 30, no. 4, pp. 1114–1128, 2022.
- [35] W. Zhang, W. Dong, M. Lv, Z. Liu, Y. Zhou, and H. Feng, "Barrier lyapunov functions-based nonsingular fixed-time switching control for strict-feedback nonlinear dynamics with full state constraints," *International Journal of Robust and Nonlinear Control*, vol. 31, no. 16, pp. 7862–7885, 2021.
- [36] B. Zhang and P. Liu, "Model-based and model-free robot control: A review," *RiTA 2020*, pp. 45–55, 2021.
- [37] L. Kong, W. He, W. Yang, Q. Li, and O. Kaynak, "Fuzzy approximation-based finite-time control for a robot with actuator saturation under time-varying constraints of work space," *IEEE Trans Cybern*, vol. 51, no. 10, pp. 4873–4884, 2021. [Online]. Available: <https://www.ncbi.nlm.nih.gov/pubmed/32721904>
- [38] Y. Hu, H. Yan, H. Zhang, M. Wang, and L. Zeng, "Robust adaptive fixed-time sliding-mode control for uncertain robotic systems with input saturation," *IEEE Trans Cybern*, vol. PP, 2022. [Online]. Available: <https://www.ncbi.nlm.nih.gov/pubmed/35442900>
- [39] D. Zhang, L. Kong, S. Zhang, Q. Li, and Q. Fu, "Neural networks-based fixed-time control for a robot with uncertainties and input deadzone," *Neurocomputing*, vol. 390, pp. 139–147, 2020. [Online]. Available: <https://www.sciencedirect.com/science/article/pii/S0925231220301247>
- [40] C. Yang, G. Peng, Y. Li, R. Cui, L. Cheng, and Z. Li, "Neural networks enhanced adaptive admittance control of optimized robot-environment interaction," *IEEE Trans Cybern*, vol. 49, no. 7, pp. 2568–2579, 2019. [Online]. Available: <https://www.ncbi.nlm.nih.gov/pubmed/29993904>
- [41] M. W. Spong, S. Hutchinson, and M. Vidyasagar, *Robot modeling and control*. John Wiley & Sons, 2020.
- [42] B. Jiang, Q. Hu, and M. I. Friswell, "Fixed-time rendezvous control of spacecraft with a tumbling target under loss of actuator effectiveness," *IEEE Transactions on Aerospace and Electronic Systems*, vol. 52, no. 4, pp. 1576–1586, 2016.
- [43] Y. Wang, Y. Song, M. Krstic, and C. Wen, "Adaptive finite time coordinated consensus for high-order multi-agent systems: Adjustable fraction power feedback approach," *Information Sciences*, vol. 372, pp. 392–406, 2016.
- [44] Z. Zuo, "Nonsingular fixed-time consensus tracking for second-order multi-agent networks," *Automatica*, vol. 54, pp. 305–309, 2015.
- [45] L. Zhang, B. Chen, C. Lin, and Y. Shang, "Fuzzy adaptive fixed-time consensus tracking control of high-order multiagent systems," *IEEE Transactions on Fuzzy Systems*, vol. 30, no. 2, pp. 567–578, 2022.
- [46] H.-q. Wang, B. Chen, and C. Lin, "Adaptive neural tracking control for a class of stochastic nonlinear systems," *International Journal of Robust and Nonlinear Control*, vol. 24, no. 7, pp. 1262–1280, 2014.
- [47] J. J. Craig, P. Hsu, and S. S. Sastry, "Adaptive control of mechanical manipulators," *The International Journal of Robotics Research*, vol. 6, no. 2, pp. 16–28, 1987.